Experimental Eye Research 174 (2018) 113–120

Contents lists available at ScienceDirect

Experimental Eye Research

journal homepage: www.elsevier.com/locate/yexer

Impact of euthanasia, dissection and postmortem delay on metabolic profile in mouse retina and RPE/choroid

Siyan Zhu[a,b], Michelle Yam[a,b], Yekai Wang[a,b], Jonathan D. Linton[c], Allison Grenell[a,b], James B. Hurley[c,d], Jianhai Du[a,b,*]

[a] Department of Ophthalmology, West Virginia University, Morgantown, WV 26506, USA
[b] Department of Biochemistry, West Virginia University, Morgantown, WV 26506, USA
[c] Department of Biochemistry, University of Washington, Seattle, WA 98109, USA
[d] Department of Ophthalmology, University of Washington, Seattle, WA 98109, USA

ARTICLE INFO

Keywords:
Metabolite
Euthanasia
Postmortem
Retina
RPE

ABSTRACT

Metabolomics studies in the retina and retinal pigment epithelium (RPE) in animal models or postmortem donors are essential to understanding the retinal metabolism and to revealing the underlying mechanisms of retinal degenerative diseases. We have studied how different methods of euthanasia (CO_2 or cervical dislocation) different isolation procedures and postmortem delay affect metabolites in mouse retina and RPE/choroid using LC MS/MS and GC MS. Compared with cervical dislocation, CO_2 exposure for 5 min dramatically degrades ATP and GTP into purine metabolites in the retina while raising intermediates in glucose metabolism and amino acids in the RPE/choroid. Isolation in cold buffer containing glucose has the least change in metabolites. Postmortem delay time-dependently and differentially impacts metabolites in the retina and RPE/choroid. In the postmortem retina, 18% of metabolites were changed at 0.5 h (h), 41% at 4 h and 51% at 8 h. However, only 6% of metabolites were changed in the postmortem RPE/choroid and it steadily increased to 20% at 8 h. Notably, both postmortem retina and RPE/choroid tissue showed increased purine metabolites. Storage of eyes in cold nutrient-rich medium substantially blocked the postmortem change in the retina and RPE/choroid. In conclusion, our study provides optimized methods to prepare fresh or postmortem retina and RPE/choroid tissue for metabolomics studies.

1. Introduction

Retina and retinal pigment epithelium (RPE) are adapted to form unique and inter-dependent metabolic pathways to efficiently utilize nutrients (Chao et al., 2017; Du et al., 2016b; Hurley et al., 2015; Kanow et al., 2017). Increasing evidence shows that the disruption of metabolism may be the basis for many retinal degenerative diseases including inherited retinal degeneration and age-related macular degeneration (AMD)(Ait-Ali et al., 2015; Ferrington et al., 2017; Geirsdottir et al., 2014; Zhang et al., 2016).

Metabolite levels and metabolic flux directly reflect the status of metabolism in biological samples. Mass spectrometry (MS) coupled with liquid chromatography (LC) or gas chromatography (GC), provides a sensitive and high-throughput platform to measure hundreds of metabolites in a single run (Cajka and Fiehn, 2016). Metabolomics studies in animal models with retinal diseases or patient postmortem tissues are extremely valuable to reveal the metabolic basis of retinal diseases and to help identify new therapeutic targets. Nevertheless, metabolomics studies in retinal tissue especially postmortem tissue are very limited. The major obstacles in these studies are when and how to harvest the samples to keep the metabolites stable during postmortem delay since metabolites are known to have rapid turnover (Dietmair et al., 2010). To investigate how postmortem influences the retinal metabolome and to study when is the best time to harvest tissue before significant metabolic change, we compared the metabolites at different times ranging from 0.5 h to 8 h in the postmortem retina and RPE/choroid. Furthermore, in this study we tested whether storage in rich culture medium could help to stabilize the metabolome.

Additionally, different methods for euthanasia and dissection techniques can contribute to variability in metabolomics studies from different labs. CO_2 and cervical dislocation are commonly used methods for euthanasia but they work by different mechanisms. CO_2 quickly blocks cellular respiration (Valentim et al., 2016) whereas cervical dislocation physically separates the head of the animal from the blood

Abbreviations: LC MS/MS, Mass spectrometry coupled with liquid chromatography; GC MS, Mass spectrometry coupled with gas chromatography; RPE, retinal pigment epithelium

* Corresponding author. WVU Eye Institute, One Medical Center Dr, PO Box 9193, Morgantown, WV 26505, USA.
E-mail address: jianhai.du@wvumedicine.org (J. Du).

https://doi.org/10.1016/j.exer.2018.05.032
Received 27 January 2018; Received in revised form 30 May 2018; Accepted 31 May 2018
Available online 01 June 2018
0014-4835/

supply and spinal column. Enucleation is one of the most widely used methods for retina isolation, but the eyes have to be dissected in buffer and the procedure can take more than 1 min. To dissect out the retina more quickly to decrease the influence of dissection time on retinal physical function, Barry Winkler developed a method to isolate a retina without enucleation. This technique has been referred to as the "Winkling" method (Anderson et al., 2002; Winkler, 1972). In this method, the retina is picked up directly from the eye within the euthanized animal after transecting the cornea and removing the lens. A retina can be isolated in as short as 15 s with this method. A disadvantage of this method is that has a higher risk of contamination by vitreous and RPE.

In this study, we combine GC MS and LC MS/MS to target metabolites, covering major metabolic pathways, and we systematically investigate how different method of euthanasia, dissection procedures and postmortem delay impact metabolites in mouse retina and RPE/choroid. Our study provides an optimized method in preparing eye samples for metabolomics and these finding will be useful for metabolomics studies in studying retinal diseases in animal models and human donors.

2. Materials and methods

2.1. Animals

C57 B6/J mice of both sexes at 6 weeks were used in this study. Mouse experiments were performed in accordance with the National Institutes of Health guidelines and the protocol approved by Institutional Animal Care and Use Committee of West Virginia University.

2.2. Retina and RPE/choroid isolation

Except for CO_2 euthanasia, all mice were euthanized through quick cervical dislocation. For CO_2 euthanasia, mice were placed in a sealed gas chamber and exposed to CO_2 at a constant flow rate at 25% of the chamber volume for 5 min, followed by cervical dislocation. Unless otherwise stated, all eyes were enucleated and submerged in 3 ml cold Hank's Balanced Salt Solution (HBSS) on ice. Upon isolation, the eye was placed under the microscope on cold HBSS-soaked filter paper. The anterior half of the eye was removed, and the posterior half was moved and submerged in a drop of 50 µl cold HBSS solution for retina isolation. Once removed, the retina was placed into a 1.5 ml microtube and snap-frozen in liquid nitrogen. The remaining RPE/choroid was cleaned by removing any lingering fat and muscle tissue then the optic nerve was removed. The sclera was not separated from the RPE/choroid to avoid the damage of RPE and shorten the time of dissection. The RPE/choroid was placed into a 2 ml microtube and snap-frozen in liquid N_2. The procedure from enucleation to snap-frozen took about 40–45 s per retina and 75–80 s per RPE/choroid.

For the Cut & Pick group ("winkling" method), after cervical dislocation, the eyeball (remaining in eye socket) was held by curved tweezers from below and the cornea was slit open using a sterilized steel blade. Gently, pressure was placed on the eyeball allowing the lens (from the cornea opening) to be exposed for removal or it was popped out. The exposed retina was removed with a clean pair of tweezers. The retina was snap-frozen in a 1.5 ml microtube in liquid N_2. The whole procedure took about 15–20 s per retina.

For the PBS experiment, HBSS was replaced by PBS for both enucleation and isolation. For postmortem delay, the eyes were stored similarly to the protocols to be used for human eye retrieval by the Royal College of Ophthalmologists (https://www.rcophth.ac.uk/standards-publications-research/clinical-guidelines/). Filter paper squares were moistened with cold PBS and placed in clean 10 mm petri dishes (1 square per dish). For each time point, eyes were enucleated and placed in the petri dishes (on top of the moist filter paper with optical nerve facing towards the paper). Dishes were sealed with parafilm and stored at 4 °C in the dark for the duration of time (0.5h, 1h, 4h and 8h). The eyes were then dissected to isolate retina and RPE/choroid. For storage in medium, the enucleated eyes were placed in a 96 well plate (1 eye per well) containing 100 µl/well DMEM/F12 (1:1) (D/F12) medium (ThermoFisher Scientific) with 10% FBS and 1% Penicillin Streptomycin. The plate was sealed with parafilm and stored at 4 °C in the dark for 8 h. Upon isolation, the eyes were transferred into 2 ml of cold HBSS to wash away the medium (3 times) before isolation.

2.3. Mass spectrometry sample preparation

Retina samples were homogenized in 140 µl cold 80% methanol (methanol:water (80:20 V/V)) using a microtube homogenizer; RPE/choroid samples were homogenized in 200 µl of cold 80% methanol using VWR 200 homogenizer. The samples were stored on dry ice for 30 min then centrifuged at 15000 RPM for 10 min. The supernatant was dried by the FreeZone 4.5 L freeze dryer (Labconco). The dried extract was either reconstituted with 100 µl of mobile phase (a mixture of A:B at 40:60 in V/V) for LC MS/MS or derivatized for GC MS.

2.4. Metabolite analysis by LC MS/MS

The extracts were analyzed by a Shimadzu LC Nexera X2 UHPLC coupled with a QTRAP 5500 LC MS/MS (AB Sciex). An ACQUITY UPLC UPLC BEH Amide analytic column (2.1 × 50 mm, 1.7 µm, Waters) was used for chromatographic separation. The mobile phase was (A) water with 10 mM ammonium acetate (pH 8.9) and (B) acetonitrile/water (95/5) with 10 mM ammonium acetate (pH 8.2) (All solvents were LC–MS Optima grade from Fisher Scientific). The total run time was 11 min with a flow rate of 0.5 ml/min with an injection volume of 5 µl. The gradient elution is 95–61% B in 6 min, 61–44% B at 8 min, 61–27% B at 8.2 min, and 27–95% B at 9 min. The column was equilibrated with 95% B at the end of each run. The source and collision gas was N_2. The ion source conditions in positive and negative mode were: curtain gas (CUR) = 25 psi, collision gas (CAD) = high, ion spray voltage (IS) = 3800/-3800 V, temperature (TEM) = 500 °C, ion source gas 1 (GS1) = 50 psi, and ion source gas 2 (GS2) = 40 psi. Each metabolite was tuned with standards for optimal transitions (Supplemental Table 1) ^{13}C-nicotinic acid (Toronto Research Chemicals) was used as the internal standard. The extracted MRM peaks were integrated using MultiQuant 3.0.2 software (AB Sciex).

2.5. Metabolite analysis by GC MS

The extracts were derivatized by methoxyamine and N-tertbutyldimethylsilyl-N-methyltrifluoroacetamide as described in detail (Chao et al., 2017; Du et al., 2015). An Agilent 7890B/5977B GC/MS system with an Agilent DB-5MS column (30 m × 0.25 mm × 0.25 µm film) was used for GC separation and analysis of metabolites. Ultra–high-purity helium was the carrier gas at a constant flow rate of 1 mL/min. One microliter of sample was injected in split-less mode by the auto sampler. The temperature gradient started at 95 °C with a hold time of 2 min and then increased at a rate of 10 °C/min to 300 °C, where it was held for 6 min. The temperatures were set as follows: inlet 250 °C, transfer line 280 °C, ion source 230 °C, and quadrupole 150 °C. Mass spectra were collected from 80 to 600 m/z under selective ion monitoring mode. Myristic acid-d27 was added into each sample as the internal standard. The data was analyzed by Agilent MassHunter Quantitative Analysis Software.

2.6. Statistical analysis

Principle component analysis (PCA) was analyzed using MetaboAnalyst (http://www.metaboanalyst.ca/). PCA is one of the most widely used multivariate analysis to differentiate between groups

in highly complex metabolomics data sets. It reduces large set of variables to much fewer variables using their weighted averages. These new variables are called scores and the weighting profiles are called loadings. The scores plot provides a visualized summary of the sample clustering patterns by projecting high-dimensional metabolomics data into two dimensions to explain the maximal variance. Scores represent the rows of X projected onto a hyperplane within the data that describes the covariances of X, or the covariances between X and Y. Groups are separated in scores only when within-class variation is less than between-class variation.

For univariate analysis, the significance of differences was determined by unpaired two-tailed t tests or analysis of variance (ANOVA) with Bonferroni post hoc test using MetaboAnalyst. Data were mean ± SD.

3. Results

3.1. Euthanasia with CO_2 significantly changes metabolites in both retina and RPE/choroid

To study the effect of euthanasia by CO_2 asphyxiation on the metabolic profile of the retina and RPE/choroid, we compared a routine euthanasia protocol of CO_2 exposure for 5 min followed by cervical dislocation compared to protocol of cervical dislocation alone (without CO_2). In both protocols the retina and RPE/choroid were isolated quickly in cold HBSS (Fig. 1A). We quantified 93 metabolites covering major metabolic pathways such as glycolysis, mitochondrial TCA cycle, amino acids, ketone bodies, cellular redox, vitamins, purine nucleotides and fatty acids by LC MS/MS and GC MS (Supplemental Table 1). Compared with the retina with cervical dislocation alone, CO_2 exposure significantly decreased high energy metabolites including phosphocreatine (P-creatine), ATP and GTP. Intermediates in glycolysis (phosphoenolpyruvate (PEP), glyceraldehyde 3-phosphate (GAP)) and mitochondrial Krebs cycle (α-ketoglutarate (α-KG) and fumarate) were decreased. Both ATP and GTP can be degraded into purine nucleotides such as AMP, inosine, hypoxanthine and xanthine (Grune et al., 1993; Swennen et al., 2008) (Fig. 1C). CO_2 exposure dramatically increased the purine nucleotides and the hypoxanthine level raised about 10 fold (Fig. 1C–D).

Surprisingly, RPE/choroid had a drastically different response to CO_2 exposure compared to the retina. 44% of the metabolites were changed in RPE/choroid, which was 3 times more than the retina (Fig. 1D). However, ATP, GTP and purine metabolites were not influenced by CO_2 exposure in the RPE/choroid. Except P-creatine and glutathione (GSH), all the altered metabolites were increased by CO_2 exposure. The γ-Aminobutyric acid (GABA) was accumulated by about 35 times with CO_2. Most amino acids and intermediates in glycolysis and Krebs cycle were increased (Fig. 1D).

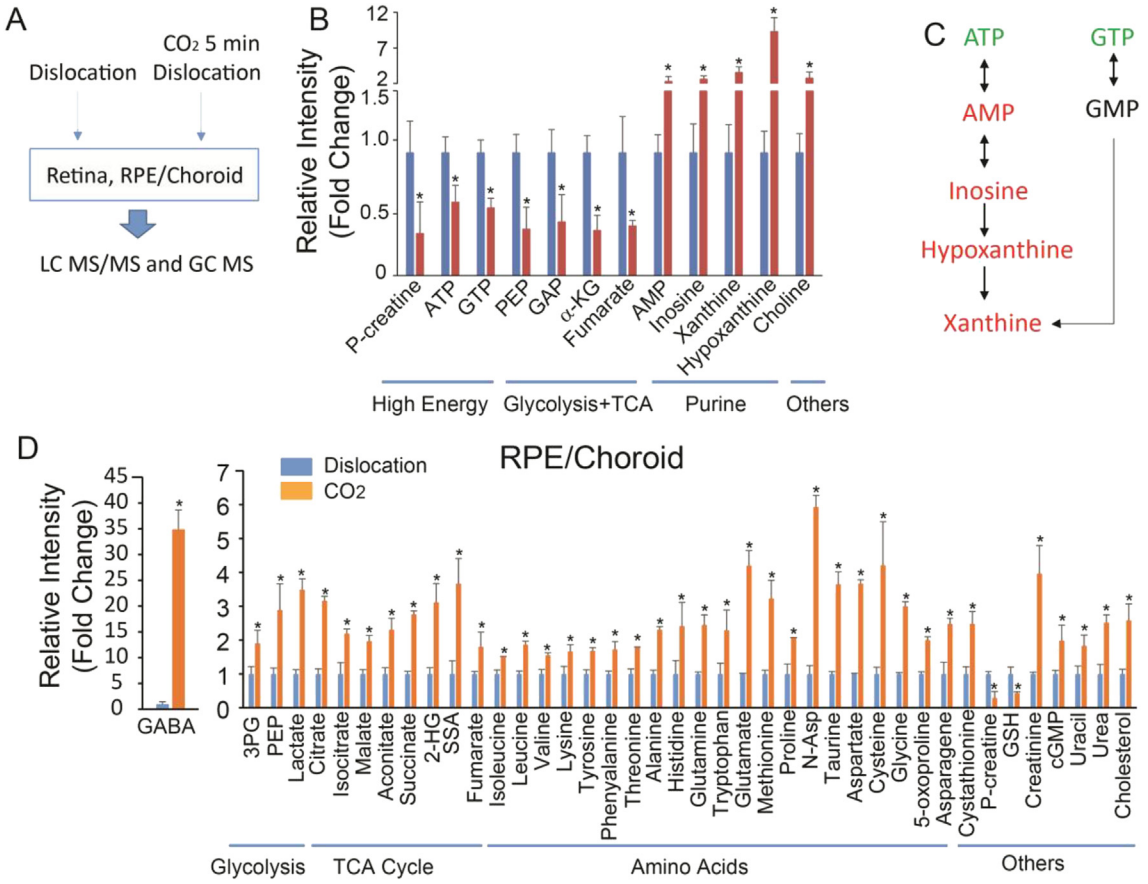

Fig. 1. The impact of euthanasia with CO_2 on metabolites in retina and RPE/choroid. (A) Schematic for experimental procedures. The mice were sacrificed by either cervical dislocation (Dislocation) or CO_2 for 5 min followed by cervical dislocation (CO_2 5 min Dislocation). The retina and RPE/choroid were isolated in cold HBSS and extracted metabolites were analyzed by mass spectrometry. (B–C) CO_2 decreased mitochondrial metabolites and promoted purine degradation in retina. Data were ion intensity normalized by those in Dislocation. *P < 0.05 with *t*-test, N = 3. High Energy, high energy phosphates. (C) A schematic for purine degradation pathway. Green represents decrease and red represents increase. (D) CO_2 impacts multiple metabolic pathways in RPE/choroid. Data were ion intensity normalized by those in Dislocation. 3 PG, 3-phosphoglycerate; PEP, phosphoenolpyruvate, 2-HG, 2-hydroxyglutarate; SSA, Succinic semialdehyde; N-ASP, N-acetylaspartate; GSH, glutathione. *P < 0.05 with *t*-Test, N = 3. (For interpretation of the references to colour in this figure legend, the reader is referred to the Web version of this article.)

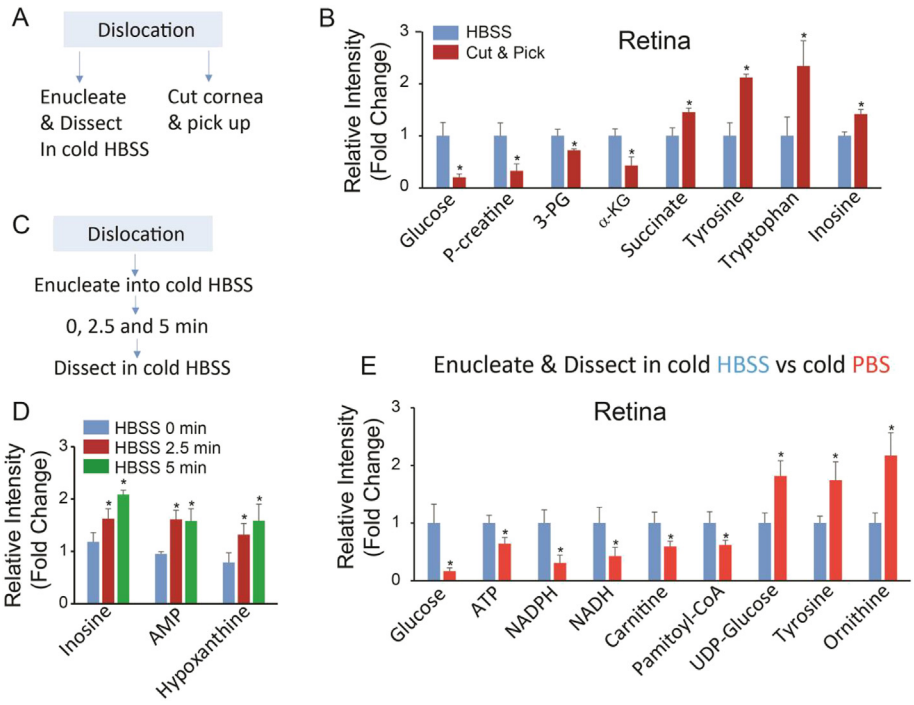

Fig. 2. The impact of isolation on metabolites in retina and RPE/choroid. (A) Schematic for different isolation procedures (See details in the methods). (B) The impact of isolation procedures on metabolites in retina. Data were normalized by the HBSS group with Enucleate & Dissect. *P < 0.05, N = 3. (C–D) The impact of short delay in cold HBSS after enucleation on metabolites in retina. The enucleated eye balls were left in cold HBSS for 0, 2.5 or 5 min before isolation in cold HBSS. *P < 0.05 vs 0 min group and #P < 0.05 vs 2.5 min group. (D) The impact of isolation procedures on metabolites in retina. Data were normalized by the HBSS group with Enucleate & Dissect. *P < 0.05, N = 3.

3.2. Different retina isolation procedures change the metabolic profile

To study how different dissection procedures affected metabolome, we compared metabolites from the retinas dissected by enucleation or "winkling" (Cut & Pick). Since it is challenging to obtain clean RPE/choroid in short time with the Cut & Pick method, we did not compare RPE/choroid with different procedures. Unexpectedly, most of the metabolites harvested by the Cut & Pick method are similar to those collected by enucleation in cold HBSS. Unexpectedly, the Cut & Pick method showed slightly decreased glucose, P-creatine, 3-phosphoglyceric acid (3-PG) and α-KG (Fig. 2A and B), suggesting that the retina has very active glucose metabolism as the Cut & Pick method was performed under room temperature.

During retina isolation, the same procedure can take different time in different labs and the eyes are often isolated separately. To investigate how short storage of enucleated eyes affects metabolites, we isolated the retina as per the common method – enucleation, then isolation and varied the time delay between enucleation and isolation. The time points were 0 min, 2.5 min and 5 min. During the time delay all eyes were stored on ice in cold HBSS. Strikingly, only three metabolites, all purine metabolites, were increased (less than 2 fold) in 2.5 min and 5 min (Fig. 2D). There were no significant different in metabolites between 2.5 min and 5 min, suggesting that storage in cold HBSS can stabilize the metabolism for a short time.

Besides HBSS, PBS is another widely used buffer for retina isolation. We compared the metabolites in retina isolated in cold HBSS or cold PBS. The major difference between HBSS and PBS is HBSS also contains 5.5 mM glucose. As expected, the retina in HBSS had 6 times more glucose than those in PBS (Fig. 2E). Despite the short isolation time, the high energy metabolites that are generated by glucose including ATP, NADPH and NADH were significantly decreased in the retina in PBS, while UDP-glucose, a key intermediate in glycogen synthesis, was accumulated (Fig. 2E).

3.3. Postmortem delay differentially alters metabolites in both retina and RPE/choroid

To examine the impact of postmortem delay on metabolites, we quickly euthanized the animals by cervical dislocation, enucleated the eyes in cold HBSS and stored the eyes in a moist environment at 4 °C in the dark as adapted from the protocols for human eye storage in the eye bank (https://www.rcophth.ac.uk/standards-publications-research/clinical-guidelines/) (Fig. 3A). In the retina, 18% of metabolites were significantly changed after storage for 0.5 h and the number of changed metabolites slightly increased to 23% after 1h. However, after 4 h and 8 h storage, the changed metabolites sharply increased to 41% and 51% respectively (Fig. 3B–C). Score plots from principle component analysis (PCA) showed all time points were different from 0 h (without delay), but there were more overlapping points between 0.5 h and 1 h (Supplemental Fig. 1), suggesting that the metabolic changes between 0.5 h and 1 h are similar. The postmortem delay in the retina time-dependently decreased the high energy metabolites, anti-oxidants and some intermediates in glucose metabolism, while most of the amino acids and purine nucleotides (Fig. 3B) were increased. Three purine metabolites (inosine, xanthine, and hypoxanthine) and two thiol-containing amino acids (cysteine and cysteine) were increased more than 10 times after 8 h.

Compared to the retina, the RPE/choroid was less sensitive to postmortem delay. Only 5% of the metabolites changed after 0.5 h, 6% after 1 h and 10% after 4 h. The maximum change was 20% after 8 h, which was much lower than the retina (Fig. 4A–B). In PCA score plots, each time point was separated from 0 h, however, there were overlapping points among 0.5 h, 1 h and 4 h and slightly overlapping between 4 h and 8 h (Supplemental Fig. 2). After 8 h, most metabolites were increased except 4-hydroxyproline and GSH. Surprisingly, ATP and P-creatine were decreased after 1 h and 4 h but increased after 8 h (Fig. 4B). The fold changes of metabolite levels were also lower than the retina. There were 5 metabolites that were increased more than 3 folds over time including xanthine and hypoxanthine which were also dramatically changed in the retina.

3.4. Storage in culture medium partially rescues the metabolic change responding to postmortem delay

To test whether storage in nutrient-rich medium could attenuate the metabolite change in postmortem delay, we stored the enucleated eyes in cold DMEM/F12 (1:1) (D/F12) medium supplemented with 10% FBS for 8 h. Compared with the retina stored in the moist environment, D/

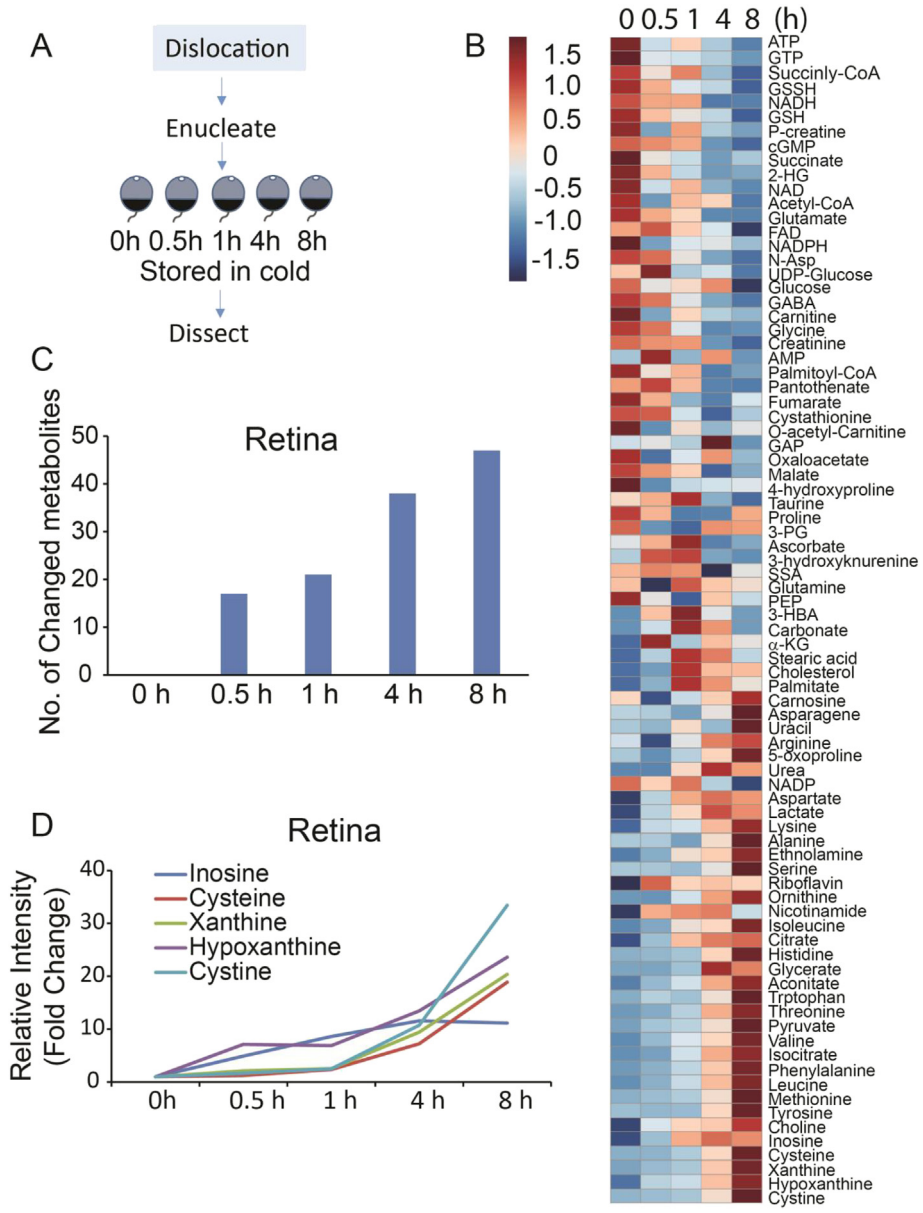

Fig. 3. The impact of postmortem delay on metabolites in retina. (A) Schematic on postmortem delay. After enucleation, the eyeballs were kept in cold moisture for different time intervals before isolation. (B) Heat map of significantly changed metabolites vs. 0 h group by One-Way ANOVA test ($P < 0.05$, $n = 3$). The data was normalized by the average from each row and clustered for similar patterns using Metaboanalyst 3.0 software. (C) The number of metabolites that were significantly changed vs. 0 h group. (D) The top changed metabolites with fold change > 10 over 0 h group. N = 3.

F12 attenuated most of the changes of acetyl-CoA, glucose and pyruvate (Fig. 5B). D/F12 medium also significantly attenuated cysteine, xanthine and hypoxanthine, which were the metabolites that changed the most during postmortem delay (Fig. 5B). Similarly, in the RPE/choroid, D/F12 medium attenuated the changes for 6 metabolites including cysteine, hypoxanthine and xanthine (Fig. 5C).

4. Discussion

Here we report how euthanasia, dissection and postmortem delay influence the metabolic profile in the retina and RPE: 1) Euthanasia with CO_2 depletes the ATP pool by inhibiting ATP generation and enhances ATP degradation in the retina. In the RPE/choroid, CO_2 increased the content of most nutrients; 2) Retina requires cold temperature and glucose during isolation to stabilize the metabolites; 3) Postmortem time-dependently and differentially influences metabolites in the retina and RPE/choroid; about 80% of metabolites are unchanged within 1 h in retina and 8 h in RPE/choroid postmortem; 4) Nutrient-rich culture medium can partially rescue the postmortem metabolic changes in both retina and RPE/choroid.

4.1. CO_2 affects metabolic profile

CO_2 inhalation is the most common method for euthanasia in mice (Valentim et al., 2016). Euthanasia with CO_2 causes diverse metabolic changes in rodent tissue (Brooks et al., 1999; Overmyer et al., 2015; Pierozan et al., 2017). In the liver and heart, the response is similar to retina wherein there is depletion of ATP and its degradation into purine metabolites (Overmyer et al., 2015). Our results in the retina are consistent with other models that disrupt the flow of oxygen to a tissue. It is known that hypoxia can accelerate the degradation of ATP and GTP into purine metabolites (Harkness and Lund, 1983; Jennings and Steenbergen, 1985). In rat retina, xanthine and hypoxanthine accumulate during transient ischemia (Roth et al., 1996, 1997). The rapid

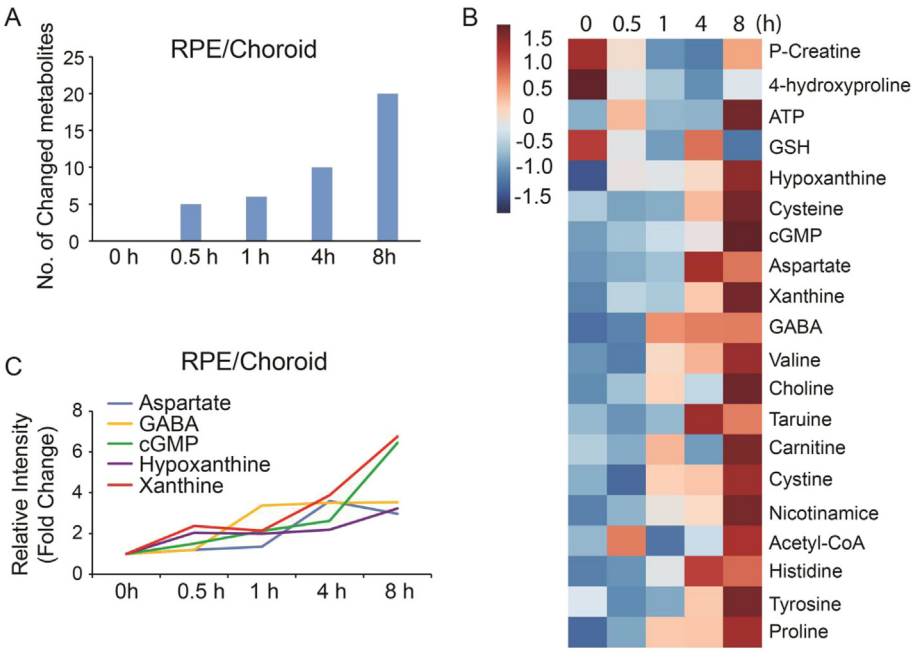

Fig. 4. The impact of postmortem delay on metabolites in RPE/choroid. (A) The number of metabolites that were significantly changed vs. 0 h group in the RPE/choroid. (B) Heat map of significantly changed metabolites vs. 0 h group by One-Way ANOVA test ($P < 0.05$, n = 3). The data was scaled by the average from each row and clustered for similar patterns using Metaboanalyst 3.0 software. (C) The top changed metabolites with fold change > 3 in the 8 h over 0 h group. N = 3.

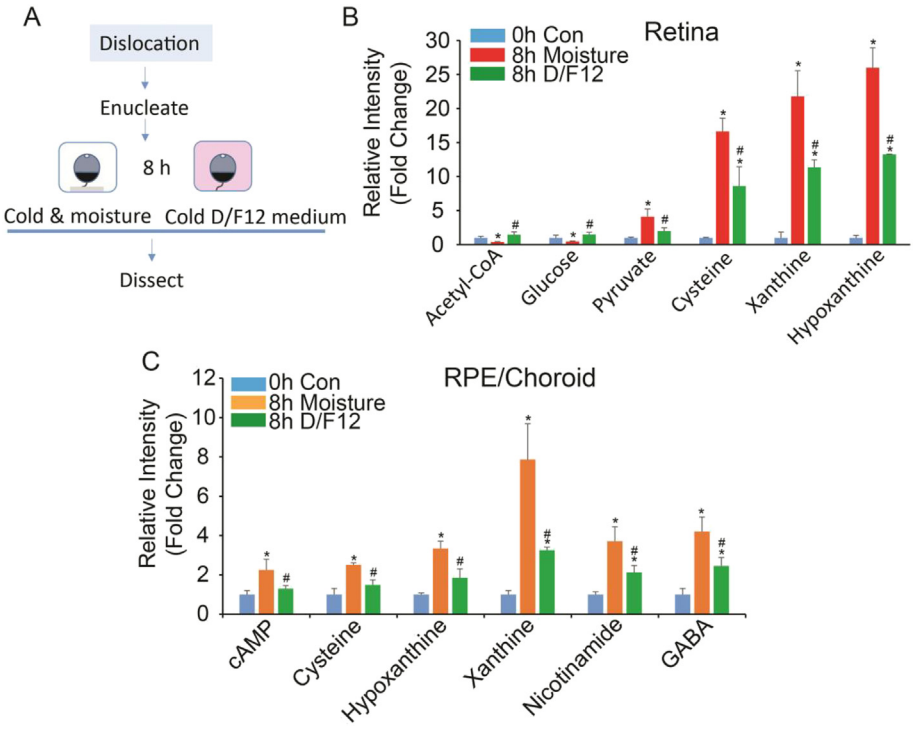

Fig. 5. D/F12 medium partially rescued the change in metabolite by postmortem delay. (A) Schematic on experiment procedures. The enucleated eyeballs were placed in either a cold and moist 96-well plate or cold D/F12 medium for 8 h before isolation. (B) D/F12 medium rescued changes of some metabolites in the retinas from storage for 8 h *P < 0.05 vs the retinas dissected at 0 h and #P < 0.05 vs the retinas storage in the moisture for 8 h by One-Way ANOVA test. N = 3. (C) D/F12 medium rescued changes of some metabolites in the RPE/choroid from stored for 8 h *P < 0.05 vs the RPE/choroid dissected at 0 h and #P < 0.05 vs the RPE/choroid stored in the moisture for 8 h by One-Way ANOVA test N = 3.

deprivation of O_2 should shut down mitochondrial oxidative phosphorylation in the retina leading to reduction of ATP and GTP. The cytosolic reducing power that could not be utilized by mitochondrial oxidation can further inhibit glycolysis. The inadequate rate to produce high energy phosphate might stimulate P-creatine to donate phosphate to ADP to generate ATP.

Comparatively, the RPE/choroid has a strikingly different metabolic response to CO_2. ATP and purine metabolites are not affected by CO_2. On the contrary, the intermediates in glycolysis and TCA cycle are increased in the RPE/choroid. This response is similar to muscle which has a stable ATP pool and enhanced glycolysis with CO_2 (Overmyer et al., 2015). The P-creatine should help to maintain ATP, since P-creatine is significantly decreased while its breakdown product creatinine is increased in the RPE/choroid (Fig. 1D). Additionally, RPE has an abundant storage of glycogen and active transporters for lactate and amino acids (Coffe et al., 2006; Hernandez et al., 2014; Lehmann et al., 2014). Exposure to CO_2 for 2.5 min could significantly stimulate enzymes in glycogen breakdown and glucose utilization (Brooks et al., 1999). RPE actively transports nutrients and intermediates to the retina and the paralysis of retinal metabolism by CO_2 may account for the nutrient accumulation in the RPE/choroid. Protein degradation might contribute to this accumulation, since most of proteinogenic amino acids are increased. However, the most dramatically changed amino acids are not proteinogenic: GABA is increased about 35 fold and N-acetyl-aspartate (N-Asp) is about 6 fold. The precursors for GABA and N-Asp, glutamate and aspartate are also dramatically increased

(Fig. 1D). These metabolites are abundant in the retina and serve as both excitatory neurotransmitters and substrates for mitochondrial TCA cycle. It is well known in the brain that excitatory amino acids are elevated and exported into other compartment during ischemia and hypoxia (Benveniste et al., 1984; Globus et al., 1988; Hagberg et al., 1985). In the cat cortex, low blood flow could cause 300-fold increase in GABA, 30-fold in glutamate and 10-fold in aspartate without change in essential amino acids (Shimada et al., 1990). We speculate that the release of these amino acids from retina may cause worsen the energy deficiency in the retina but energy surplus in the RPE during CO_2 exposure. These findings may shed the light in understanding the metabolism in ischemic retinal diseases.

4.2. The importance of low temperature and glucose availability in isolation

Mouse retina has extremely fast metabolism. We previously reported that more than 50% of the ^{12}C glycolytic intermediates were replaced by ^{13}C intermediates from ^{13}C glucose in 5 min (Du et al., 2013). With light illumination within minutes, cGMP falls 5 times and mitochondrial O_2 consumption drops (Du et al., 2016a). Our observation that retina isolated in cold HBSS has higher intermediates in glucose metabolism than those of the Cut & Pick method supports the notion that the cold temperature is critical to quench the metabolism in retina isolation. However, the ice-cold buffer does not stop metabolism. When isolated in cold PBS, retinas had significantly lower ATP, NADPH and NADH compared those in cold HBSS. This result suggests that retinal metabolism is still active in cold medium and glucose is required in the buffer to avoid the stress of fuel shortage. However, we cannot exclude the possibility that the surrounding HBSS may provide the retina more access to glucose than they ever receive in the eye, which is limited by the blood flow. Since, current processes cannot measure *in vivo* metabolite concentration in real time, we speculate that these levels of high energy metabolites *in vivo* is likely to reflect a range between our results from cold HBSS and Cut & Pick.

4.3. Postmortem delay differentially impacts metabolic profile in retina and RPE/choroid

In our study, postmortem delay time-dependently impacts the retinal metabolites as early as 0.5 h with 18% of changed metabolites. However, a recent study by Tan et al. (2016) reported that metabolites in the rat retina were stable for 8 h postmortem, except the increase of some TCA intermediates after 2 h. This discrepancy can be attributed to the following factors; 1) Tan et al. used CO_2 to euthanize before cervical dislocation. We have shown CO_2 can substantially increase the purine metabolites, which also rise in the postmortem retina. Euthanasia with CO_2 can overshadow the changes of these metabolites. 2) The isolation time for each retina in their study varied between 1 and 20 min in an unspecified buffer. Each of the postmortem retinas in our study was isolated in less than 45 s in cold HBSS. 3) The LC-MS/MS method we use is more sensitive and quantitative. For example, we found substantial decreases of ATP, GTP, NAD and NADPH in 0.5 h, but Tan et al. did not detect these metabolites in retinas in their assay.

Purine metabolites are the most common and most substantially elevated metabolites in postmortem retina and RPE/choroid. The increase of hypoxanthine in postmortem vitreous is well known and has been used as a marker to estimate the postmortem interval (James et al., 1997; Madea et al., 1994; Madea and Rodig, 2006; Munoz et al., 2006). The storage of eyes in nutrient-rich medium significantly blocks the elevation of purine metabolites, suggesting that there is still an energy demand when eyes are stored in the cold. Future investigations will be needed to study whether more exposure to medium such as poking a hole or slicing open the eye would provide better prevention of metabolic change.

Why are there much more substantial changes of metabolites in the postmortem retina than RPE/choroid? We speculate that the retina has a more active metabolism but it has no direct access to nutrients. However, the RPE/choroid is surrounded with a reservoir of nutrients, which may sustain them from the short postmortem effect. Therefore, ATP and other high energy metabolites are being depleted starting at 0.5 h in the retina while these metabolites are stable or even higher at 8 h in RPE/choroid. For a stable and reliable metabolite study in postmortem eye sample, our data suggest that the retina samples have to be collected within 1 h but RPE/choroid samples can be collected as late as 4 h even 8 h postmortem.

4.4. Limitations and future research

Cervical dislocation is a rapid method for euthanasia but it still causes loss of blood circulation before tissue harvest. Other methods in tissue harvest without disturbing blood flow like anesthesia should be compared in the future. In this study, the tissues are snap frozen in liquid nitrogen which may not completely quench the metabolism. It is possible that the metabolites can change while samples are frozen. Other faster quenching methods including freeze-clamping and microwave radiation (Belanger et al., 2002; Detour et al., 2011) can be studied in future research. Additionally, since the enriched DMEM/F12 could not rescue most other metabolites, investigation of other storage media or conditions are required.

In conclusion, we have tested how euthanasia, isolation and postmortem impact the stability of metabolites in the mouse retina and RPE. Our results recommend an optimized sample preparation for metabolite study: 1) avoid CO_2 in euthanasia; 2) isolate quickly in cold HBSS; 3) store postmortem eyes in culture medium at 4 °C in the dark; 4) discretion in data interpretation for postmortem eyes. It is also recommended that the retina should be harvested within 1 h and RPE/choroid should be harvested within 8 h after death, to enable the stability of 80% of major metabolites.

Conflicts of interest

None declared.

Author contributions

Conceptualization, S.Z. and J.D; Investigation, S.Z., M.Y., Y.W., J.D.L., A.G., and J.D.; Writing, S.Z., M.Y., Y.W., J.B.H., and J.D.; Funding Acquisition, J.B.H., and J.D; Supervision, J.B.H., and J.D.

Acknowledgements

This work was supported by NIH Grants EY026030 (to J.D., and Jennifer Chao.), EY06641 (to J.B.H.), EY017863 (to J.B.H.), and the BrightFocus Foundation M2016047 (to J.D.).We thank Connor Jankowski from Dr. Hurley lab for helping with the metabolite extraction in the isolation of retinas in PBS.

Appendix A. Supplementary data

Supplementary data related to this article can be found at http://dx.doi.org/10.1016/j.exer.2018.05.032.

References

Ait-Ali, N., Fridlich, R., Millet-Puel, G., Clerin, E., Delalande, F., Jaillard, C., Blond, F., Perrocheau, L., Reichman, S., Byrne, L.C., Olivier-Bandini, A., Bellalou, J., Moyse, E., Bouillaud, F., Nicol, X., Dalkara, D., van Dorsselaer, A., Sahel, J.A., Leveillard, T., 2015. Rod-derived cone viability factor promotes cone survival by stimulating aerobic glycolysis. Cell 161, 817–832.

Anderson, R.E., Maude, M.B., McClellan, M., Matthes, M.T., Yasumura, D., LaVail, M.M., 2002. Low docosahexaenoic acid levels in rod outer segments of rats with P23H and S334ter rhodopsin mutations. Mol. Vis. 8, 351–358.

Belanger, M.P., Askin, N., Wittnich, C., 2002. Multiple in vivo liver biopsies using a freeze-clamping technique. J. Invest. Surg.: Offic. J. Acad. Surg. Res. 15, 109–112.

Benveniste, H., Drejer, J., Schousboe, A., Diemer, N.H., 1984. Elevation of the extracellular concentrations of glutamate and aspartate in rat hippocampus during transient cerebral ischemia monitored by intracerebral microdialysis. J. Neurochem. 43, 1369–1374.
Brooks, S.P., Lampi, B.J., Bihun, C.G., 1999. The influence of euthanasia methods on rat liver metabolism. Contemp. Top. Lab. Anim. Sci. 38, 19–24.
Cajka, T., Fiehn, O., 2016. Toward merging untargeted and targeted methods in mass spectrometry-based metabolomics and lipidomics. Anal. Chem. 88, 524–545.
Chao, J.R., Knight, K., Engel, A.L., Jankowski, C., Wang, Y., Manson, M.A., Gu, H., Djukovic, D., Raftery, D., Hurley, J.B., Du, J., 2017. Human retinal pigment epithelial cells prefer proline as a nutrient and transport metabolic intermediates to the retinal side. J. Biol. Chem. 292, 12895–12905.
Coffe, V., Carbajal, R.C., Salceda, R., 2006. Glucose metabolism in rat retinal pigment epithelium. Neurochem. Res. 31, 103–108.
Detour, J., Elbayed, K., Piotto, M., Moussallieh, F.M., Nehlig, A., Namer, I.J., 2011. Ultrafast in vivo microwave irradiation for enhanced metabolic stability of brain biopsy samples during HRMAS NMR analysis. J. Neurosci. Meth. 201, 89–97.
Dietmair, S., Timmins, N.E., Gray, P.P., Nielsen, L.K., Kromer, J.O., 2010. Towards quantitative metabolomics of mammalian cells: development of a metabolite extraction protocol. Anal. Biochem. 404, 155–164.
Du, J., Cleghorn, W., Contreras, L., Linton, J.D., Chan, G.C., Chertov, A.O., Saheki, T., Govindaraju, V., Sadilek, M., Satrustegui, J., Hurley, J.B., 2013. Cytosolic reducing power preserves glutamate in retina. Proc. Natl. Acad. Sci. U. S. A 110, 18501–18506.
Du, J., Linton, J.D., Hurley, J.B., 2015. Probing metabolism in the intact retina using stable isotope tracers. Meth. Enzymol. 561, 149–170.
Du, J., Rountree, A., Cleghorn, W.M., Contreras, L., Lindsay, K.J., Sadilek, M., Gu, H., Djukovic, D., Raftery, D., Satrustegui, J., Kanow, M., Chan, L., Tsang, S.H., Sweet, I.R., Hurley, J.B., 2016a. Phototransduction influences metabolic flux and nucleotide metabolism in mouse retina. J. Biol. Chem. 291, 4698–4710.
Du, J., Yanagida, A., Knight, K., Engel, A.L., Vo, A.H., Jankowski, C., Sadilek, M., Tran, V.T., Manson, M.A., Ramakrishnan, A., Hurley, J.B., Chao, J.R., 2016b. Reductive carboxylation is a major metabolic pathway in the retinal pigment epithelium. Proc. Natl. Acad. Sci. U. S. A 113, 14710–14715.
Ferrington, D.A., Ebeling, M.C., Kapphahn, R.J., Terluk, M.R., Fisher, C.R., Polanco, J.R., Roehrich, H., Leary, M.M., Geng, Z., Dutton, J.R., Montezuma, S.R., 2017. Altered bioenergetics and enhanced resistance to oxidative stress in human retinal pigment epithelial cells from donors with age-related macular degeneration. Redox biology 13, 255–265.
Geirsdottir, A., Hardarson, S.H., Olafsdottir, O.B., Stefansson, E., 2014. Retinal oxygen metabolism in exudative age-related macular degeneration. Acta Ophthalmol. 92, 27–33.
Globus, M.Y., Busto, R., Dietrich, W.D., Martinez, E., Valdes, I., Ginsberg, M.D., 1988. Effect of ischemia on the in vivo release of striatal dopamine, glutamate, and gamma-aminobutyric acid studied by intracerebral microdialysis. J. Neurochem. 51, 1455–1464.
Grune, T., Schneider, W., Siems, W.G., 1993. Reoxygenation injury of rat hepatocytes: evaluation of nucleotide depletion and oxidative stress as causal components. Cell. Mol. Biol. 39, 635–650.
Hagberg, H., Lehmann, A., Sandberg, M., Nystrom, B., Jacobson, I., Hamberger, A., 1985. Ischemia-induced shift of inhibitory and excitatory amino acids from intra- to extracellular compartments. J. Cerebr. Blood Flow Metabol.: Offic. J. Int. Soc. Cerebr. Blood Flow Metabol. 5, 413–419.
Harkness, R.A., Lund, R.J., 1983. Cerebrospinal fluid concentrations of hypoxanthine, xanthine, uridine and inosine: high concentrations of the ATP metabolite, hypoxanthine, after hypoxia. J. Clin. Pathol. 36, 1–8.
Hernandez, C., Garcia-Ramirez, M., Garcia-Rocha, M., Saez-Lopez, C., Valverde, A.M., Guinovart, J.J., Simo, R., 2014. Glycogen storage in the human retinal pigment epithelium: a comparative study of diabetic and non-diabetic donors. Acta Diabetol. 51, 543–552.
Hurley, J.B., Lindsay, K.J., Du, J., 2015. Glucose, lactate, and shuttling of metabolites in vertebrate retinas. J. Neurosci. Res. 93, 1079–1092.
James, R.A., Hoadley, P.A., Sampson, B.G., 1997. Determination of postmortem interval by sampling vitreous humour. Am. J. Forensic Med. Pathol 18, 158–162.
Jennings, R.B., Steenbergen Jr., C., 1985. Nucleotide metabolism and cellular damage in myocardial ischemia. Annu. Rev. Physiol. 47, 727–749.
Kanow, M.A., Giarmarco, M.M., Jankowski, C.S., Tsantilas, K., Engel, A.L., Du, J., Linton, J.D., Farnsworth, C.C., Sloat, S.R., Rountree, A., Sweet, I.R., Lindsay, K.J., Parker, E.D., Brockerhoff, S.E., Sadilek, M., Chao, J.R., Hurley, J.B., 2017. Biochemical adaptations of the retina and retinal pigment epithelium support a metabolic ecosystem in the vertebrate eye. eLife 6.
Lehmann, G.L., Benedicto, I., Philp, N.J., Rodriguez-Boulan, E., 2014. Plasma membrane protein polarity and trafficking in RPE cells: past, present and future. Exp. Eye Res. 126, 5–15.
Madea, B., Kaferstein, H., Hermann, N., Sticht, G., 1994. Hypoxanthine in vitreous humor and cerebrospinal fluid–a marker of postmortem interval and prolonged (vital) hypoxia? Remarks also on hypoxanthine in SIDS. Forensic Sci. Int. 65, 19–31.
Madea, B., Rodig, A., 2006. Time of death dependent criteria in vitreous humor: accuracy of estimating the time since death. Forensic Sci. Int. 164, 87–92.
Munoz, J.I., Costas, E., Rodriguez-Calvo, M.S., Suarez-Penaranda, J.M., Lopez-Rivadulla, M., Concheiro, L., 2006. A high-performance liquid chromatography method for hypoxanthine determination in vitreous humour: application to estimation of post mortem interval. Hum. Exp. Toxicol. 25, 279–281.
Overmyer, K.A., Thonusin, C., Qi, N.R., Burant, C.F., Evans, C.R., 2015. Impact of anesthesia and euthanasia on metabolomics of mammalian tissues: studies in a C57BL/6J mouse model. PLoS One 10, e0117232.
Pierozan, P., Jerneren, F., Ransome, Y., Karlsson, O., 2017. The choice of euthanasia method affects metabolic serum biomarkers. Basic Clin. Pharmacol. Toxicol. 121, 113–118.
Roth, S., Osinski, J.V., Park, S.S., ostwald, P., Moshfeghi, A.A., 1996. Measurement of purine nucleoside concentration in the intact rat retina. J. Neurosci. Meth. 68, 87–90.
Roth, S., Rosenbaum, P.S., Osinski, J., Park, S.S., Toledano, A.Y., Li, B., Moshfeghi, A.A., 1997. Ischemia induces significant changes in purine nucleoside concentration in the retina-choroid in rats. Exp. Eye Res. 65, 771–779.
Shimada, N., Graf, R., Rosner, G., Heiss, W.D., 1990. Differences in ischemia-induced accumulation of amino acids in the cat cortex. Stroke 21, 1445–1451.
Swennen, E.L., Coolen, E.J., Arts, I.C., Bast, A., Dagnelie, P.C., 2008. Time-dependent effects of ATP and its degradation products on inflammatory markers in human blood ex vivo. Immunobiology 213, 389–397.
Tan, S.Z., Mullard, G., Hollywood, K.A., Dunn, W.B., Bishop, P.N., 2016. Characterisation of the metabolome of ocular tissues and post-mortem changes in the rat retina. Exp. Eye Res. 149, 8–15.
Valentim, A.M., Guedes, S.R., Pereira, A.M., Antunes, L.M., 2016. Euthanasia using gaseous agents in laboratory rodents. Lab. Anim 50, 241–253.
Winkler, B.S., 1972. The electroretinogram of the isolated rat retina. Vis. Res. 12, 1183–1198.
Zhang, L., Du, J., Justus, S., Hsu, C.W., Bonet-Ponce, L., Wu, W.H., Tsai, Y.T., Wu, W.P., Jia, Y., Duong, J.K., Mahajan, V.B., Lin, C.S., Wang, S., Hurley, J.B., Tsang, S.H., 2016. Reprogramming metabolism by targeting sirtuin 6 attenuates retinal degeneration. J. Clin. Invest. 126, 4659–4673.